arXiv:1011.0145v2 [astro-ph.HE] 5 May 2011

Modeling the Multi-Wavelength Emission of Shell-Type Supernova Remnant RX J1713.7-3946

Qiang Yuan[1], Siming Liu[2,3], Zhonghui Fan[4], Xiaojun Bi[1,5], and Christopher L. Fryer[6,7]

[1] *Key Laboratory of Particle Astrophysics, Institute of High Energy Physics, Chinese Academy of Sciences, Beijing 100049, P. R. China*
[2] *Department of Physics and Astronomy, University of Glasgow, Glasgow G12 8QQ, UK*
[3] *Key Laboratory of Dark Matter and Space Astronomy, Purple Mountain Observatory, Chinese Academy of Sciences, Nanjing 210008, P. R. China*
[4] *Department of Physics, Yunnan University, Kunming 650091, Yunnan, P. R. China*
[5] *Center for High Energy Physics, Peking University, Beijing 100871, P.R.China*
[6] *Los Alamos National Laboratories, Los Alamos, NM 87545*
[7] *Physics Department, University of Arizona, Tucson AZ 85721*

ABSTRACT

Emission mechanisms of the shell-type supernova remnant (SNR) RX J1713.7-3946 are studied with multi-wavelength observational data from radio, X-ray, GeV γ-ray to TeV γ-ray band. A Markov Chain Monte Carlo method is employed to explore the high-dimensional model parameter space systematically. Three scenarios for the γ-ray emission are investigated: the leptonic, the hadronic and a hybrid one. Thermal emission from the background plasma is also included to constrain the gas density, assuming ionization equilibrium, and a 2σ upper limit of about 0.03 cm^{-3} is obtained as far as thermal energies account for a significant fraction of the dissipated kinetic energy of the SNR shock. Although systematic errors dominate the χ^2 of the spectral fit of all models, we find that 1) the leptonic model has the best constrained model parameters, whose values can be easily accommodated with a typical supernova, but gives relatively poor fit to the TeV γ-ray data; 2) The hybrid scenario has one more parameter than the leptonic one and improves the overall spectral fit significantly; 3) The hadronic one, which has three more parameters than the leptonic model, gives the best fit to the overall spectrum with relatively not-well-constrained model parameters and very hard spectra of accelerated particles. The uncertainties of the model parameters decrease significantly if the spectral indices of accelerated electrons and protons are the same. The hybrid and hadronic models also require an energy input into high-energy protons, which seems to be too high compared with typical values of a supernova explosion. Further investigations are required to reconcile these observations with SNR theories.

Subject headings: radiation mechanism: non-thermal — ISM: supernova remnants — cosmic rays — Gamma rays: ISM

1. Introduction

Supernova remnants (SNRs) are widely thought to be one important kind of cosmic ray (CR) sources in the Galaxy (Aharonian et al. 2004). The most direct evidence comes from high-energy γ-ray emission from SNRs. Generally there are two types of scenarios for production of high energy γ-rays: the leptonic (via inverse Compton scattering of background photos by relativistic electrons) and hadronic (via decay of neutral pions produced by elastic collisions of relativistic ions with ions in the background plasma) origins. Understanding which of these two scenarios is dominant in specific sources is very important for the search of CR nuclei sources and the study of CR acceleration (Gabici 2008).

Usually it is difficult to distinguish the leptonic model and hadronic model just with the high energy γ-ray data alone. Multi-wavelength observations of photon emission from SNRs can provide us key information about the radiation mechanism. Shell-type SNR RX J1713.7-3946 is one of the most widely studied SNRs with perhaps the best multi-wavelength observations. The observational data span from radio (Lazendic et al. 2004), infrared (Benjamin et al. 2003; Acero et al. 2009), X-ray (Koyama et al. 1997; Uchiyama et al. 2003; Cassam-Chenaï et al. 2004), GeV γ-ray (Abdo et al. 2011), to TeV γ-ray band (Muraishi et al. 2000; Enomoto et al. 2002; Aharonian et al. 2006). Recent observations, especially the X-ray emission detected by *Suzaku* (Tanaka et al. 2008) and TeV γ-ray emission measured by *HESS* (Aharonian et al. 2007), give the energy spectra and images of this SNR with very high quality, which makes detailed modelings of the emission mechanism plausible (Morlino et al. 2009a; Fang et al. 2009; Fan et al. 2010a; Zirakashvili & Aharonian 2010; Ellison et al. 2010; Fan et al. 2010b). The newly reported data from *Fermi* (Abdo et al. 2011) also set strict constraints on the nature of the radiation from this SNR.

Basic results of recent studies of this SNR may be summarized briefly as the following. The wide range TeV γ-ray spectrum favors a hadronic origin of the high energy emission (Aharonian et al. 2006; Drury et al. 2009; Morlino et al. 2009a; Fang et al. 2009; Berezhko & Völk 2010). This scenario is also in line with the long standing view that SNRs are the most important CR accelerators (Axford 1981). However, there is a strong correlation between the X-ray image and TeV γ-ray image, favoring a leptonic origin of the multi-wavelength emission (Aharonian et al. 2006; Acero et al. 2009). Plaga (2008) also claims that the lack of spatial correlation between γ-rays and the molecular cloud in the vicinity of SNR RX J1713.7-3946 argues against the hadronic scenario. Furthermore the lack of thermal line emission on the X-ray spectrum sets an upper limit on the ambient plasma density of about 0.02 cm^{-3} (Cassam-Chenaï et al. 2004), which implies a very high energy content of accelerated protons from the supernova explosion. The hadronic model actually has a proton acceleration efficiency more than 4 orders of magnitude higher than the electron acceleration efficiency, which corresponds to a rather extreme scenario (Butt et al. 2008). It has been shown that the leptonic model can reproduce the multi-wavelength data and the model parameters can be easily accommodated by typical SNRs (Zirakashvili & Aharonian 2010; Ellison et al. 2010) though the overall fit to the data is relatively poor for the simplest cases. The spectral fit can be improved by considering details of electron acceleration near the high energy cutoff (Liu et al. 2008; Fan et al. 2010a,b). In fact, the cutoff of the TeV spectrum at a few tens of TeV favors the leptonic model since production of photons at even higher energies through inverse Comptonization of the cosmic microwave radiation by TeV electrons is in the Klein-Nishina regime and therefore very inefficient (Gabici 2008). The observed decay of bright X-ray filaments with a width of ~ 0.1 lyr on a timescale of ~ 1 year, on the other hand, can be attributed to fast diffusion of high energy electrons in a weak magnetic field away from intermittently formed regions of relatively high accelerated electron density (Uchiyama et al. 2007; Liu et al. 2008).

It is evident that even with both theoretical and observational advances on this source recently, the nature of the TeV emission is still inconclusive. The multi-wavelength observational data justifies a systematic modeling of the emission spectrum. Moreover, the thermal emission needs to be taken into account to get more quantitative constraints. This paper focuses on these two aspects. Fan et al. (2010b) studied the goodness-of-fit for various physically motivated leptonic models and found that the diffusive shock acceleration and the stochastic acceleration give comparably good fits. In this work we generalize this analysis by including the hadronic component. We employ the Markov Chain Monte Carlo (MCMC) method to constrain the model parameters, and investigate the full, correlated parameter space systematically. The non-thermal spectra of CR electrons and/or protons are parameterized in the simplest way, i.e., a power law with a high-energy cutoff. The thermal bremmstrahlung radiation and line emission of the background plasma are also taken into account in the fit. We consider three scenarios for the γ-ray emission, the purely leptonic model, the hadronic model and a hybrid model where the number of model parameters is reduced by requiring the spectral parameters of CR protons and electrons are identical except the normalization (see Sec. 2. below). The fitting results are presented in Section 2 and show consistency with previous studies. The conclusion is drawn in Section 3, where we also discuss possible future researches necessary to improve our understanding of this source.

2. Fitting results

In this section, we use the MCMC technique to constrain the model parameters. The MCMC method is well suitable for high dimensional parameter space investigation. The Metropolis-Hastings algorithm is used when sampling the model parameters. The probability density distributions of the model parameters can also be simply approximated by the number density of the sample points. A brief introduction to the basic procedure of the MCMC sampling can be found in Fan et al. (2010b). For more details about the MCMC method, please refer to Neal (1993); Gamerman (1997); Mackay (2003).

We also discuss implications of model parameters from the best fits to multi-wavelength data of SNR RX J1713.7-3946 for three scenarios of the γ-ray emission. In all these scenarios, the radio to X-ray emissions are generated through synchrotron of relativistic electrons. The high energy γ-rays are produced with different mechanisms. The basic physical parameters of SNR RX J1713.7-3946 are adopted as: Age $T_{\rm life} \approx 1600$ yr, Distance $d \approx 1$ kpc, and Radius $R \approx 10$ pc (Wang et al. 1997), and we assume a uniform emission sphere with a radius of R in deriving related quantities. Although the errors of the Fermi data are large, we still include these data in the spectral fits (Abdo et al. 2011). The procedure described in this paper can be applied to future observations with improved data to evaluate different emission models.

2.1. Leptonic scenario

In the leptonic scenario the γ-ray emission is produced through inverse Compton (IC) scattering of energetic electrons off the background radiation field, including the interstellar infrared, optical radiation, and the cosmic microwave background (CMB). The energy spectrum of accelerated electrons is prescribed as $F_e(E) \propto E^{-\alpha_e} \exp\left[-(E/E_c^e)^{\delta_e}\right]$, where E, α_e, E_c^e are the electron energy, power law spectral index, high-energy cutoff energy, respectively, and δ_e describes the sharpness of this cutoff. The normalization is given through the total energy of electrons above 1 GeV, W_e. The synchrotron radiation also depends on the magnetic field strength B.

The interstellar radiation field (ISRF) other than the CMB may be important for the calculation of IC γ-ray spectrum. The inclusion of ISRF has been proposed to improve the fit to the *HESS* data (Porter et al. 2006). However, given the new data of X-ray by *Suzaku* and TeV γ-ray by *HESS*, it was shown that only if the intensity of ISRF is artificially boosted by more than one order of magnitude, the goodness-of-fit can be improved significantly (Tanaka et al. 2008; Morlino et al. 2009a). In this work the ISRF is adopted as that given by Porter et al. (2006) at a distance of 7.5 kpc from the Galactic center and in the equatorial plane of the Galactic disk (Moskalenko et al. 2006). Our results are not sensitive to details of the ISRF.

Thermal X-ray emission mostly depends on the density of the shocked interstellar medium (ISM) $n_{\rm ISM}$ and the temperature of background electrons T_e. Depending on the effect of accelerated particles on the shock structure, the density is a factor of a few higher than the density in the un-shocked upstream region (Berezhko & Ellison 1999; Warren et al. 2005). The electron temperature due to Coulomb collisional energy exchange with ions is estimated by Hughes et al. (2000); Fan et al. (2010a)

$$T_e > 2.1 \times 10^7 \left(\frac{T_{\rm life}}{1600\,{\rm yr}}\right)^{2/5} \left(\frac{n_{\rm ISM}}{{\rm cm}^{-3}}\right)^{2/5} \left(\frac{T_i}{1.3 \times 10^8\,{\rm K}}\right)^{2/5}, \tag{1}$$

where T_i is the temperature of background ions. T_i is estimated to be higher than $\sim 1.3 \times 10^8$ K if the background is heated by the shock (Fan et al. 2010a). For $n_{\rm ISM} \approx 0.02$ cm^{-3}, T_e should be higher than 4×10^6 K. Drury et al. (2009) alternatively proposed that the post-shock region temperature could be reduced significantly in the case of large Mach number of the shock and effective particle acceleration. If this is the case, as we will show below, the constraint on the density and therefore the relativistic proton energy in the hadronic and hybrid models will be less strict. However, there are still significant uncertainties in the plasma heating downstream (Ghavamian et al. 2007; Gabici 2008), and it was also argued that such an extreme condition was not easy to meet and the post-shock plasma should be heated more strongly (Ellison et al. 2010). Since there is no direct constraint on T_e due to the lack of thermal emission, instead of including T_e in the MCMC fit, we take some typical values of T_e. For the sake of simplicity, we assume that the background electrons are in ionization equilibrium with the background ions and use the Raymond-Smith plasma code to calculate the thermal emission for given $n_{\rm ISM}$, T_e and the metalicity (Raymond & Smith 1977). The emission includes the recombination, bremmstrahlung, two photon process, and line emissions. The chemical abundance of the ISM is taken from Allen (1973). For emission lines lying in the energy range of X-ray data ($0.5 - 33$ keV), we convolve the model spectrum with a Gaussian energy spread function, whose width is adopted as the characteristic energy resolution of *Suzaku* (Koyama et al. 2007).

In total there are 6 free parameters, α_e, E_c^e, W_e, δ_e, B, and $n_{\rm ISM}$ in the lepton model. The 1-dimensional (1-D) probability distributions and 2-dimensional (2-D) confidence regions (at 1σ and 2σ confidence levels) of the model parameters, and the best-fit spectral energy distribution (SED) of the source are shown in Fig. 1. The best fit model parameters correspond to the peak of the 1-D probability distributions. The spectral parameters in the leptonic scenario are well constrained except for $n_{\rm ISM}$, whose 2σ upper limit is well

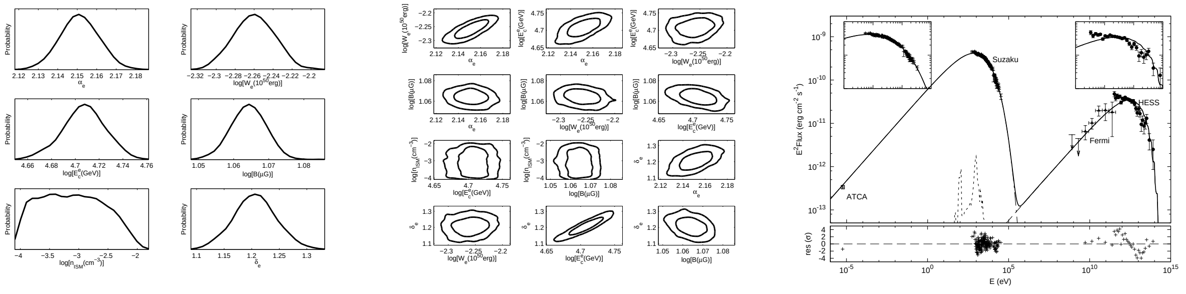

Fig. 1.— Left: 1-D probability distribution of the parameters in the leptonic model; Middle: 2-D confidence contours of the parameters. The contours are for 1 and 2 σ levels; Right: the best fit to the spectral energy distribution (SED) from radio (Acero et al. 2009), X-ray (Tanaka et al. 2008), GeV γ-ray (Abdo et al. 2011) and TeV γ-ray observations (Aharonian et al. 2007). The background electron temperature is 10^7 K. The thermal emission component indicated by the dotted line corresponds to the 2σ upper limit of 0.007 cm^{-3} for n_{ISM}.

determined. In this calculation we set $T_e = 10^7$ K. The only parameter sensitive to T_e is n_{ISM} in the leptonic scenario. The 2σ upper limit of n_{ISM} is 0.007 cm^{-3} for $T_e = 10^7$ K. The dotted line in the right panel of Fig. 1 indicates the thermal emission for these parameters. Since the ISM density will be more essential for the discussion of the hybrid and hadronic models, we will discuss the T_e dependence of these results in detail in the subsection 2.4.

For the 2-D confidence regions of the parameters, we only show combinations with relatively large correlation. There are very weak correlations among α_e, E_c^e, W_e and B. The weak correlation between α_e and W_e is mostly due to the facts that electrons near the high-energy cutoff are well-constrained by observations and low-energy electrons contribute the most to W_e for $\alpha_e > 2$. The correlation between δ_e and E_c^e is caused by the well observed spectral shape in hard X-rays and TeV γ-rays. The combination of the X-ray and γ-ray data helps to determine the model parameters. In the following we will see that X-ray data alone lead to poorly constrained and highly correlated parameters. This is an example to show the importance of global fit to the multi-wavelength data.

The parameters and χ^2 values of the best fit model are compiled in Tables 1 and 2, respectively. Since n_{ISM} is not well constrained, its 2σ upper limit instead of the best fit value is listed in Table 1. The best-fit parameters are consistent with previous studies (Aharonian et al. 2006; Liu et al. 2008; Tanaka et al. 2008) and can be readily accommodated with typical SNRs (Ellison et al. 2010). The overall χ^2 of the fit is relatively large with the reduced $\chi^2 \sim 466.9/232 = 2.01$. Such a high value of χ^2 shows that systematic errors dominate. This is not surprising given the relatively complex structure of the SNR, uncertainties related to the particle acceleration process, and our rather simple prescription of the emission model. The systematic errors actually dominate in all emission models, which is typical for modeling of astrophysical observations of relatively complex phenomena. The X-ray and TeV γ-ray data contribute the most to the overall χ^2. Especially for the TeV γ-ray data, the χ^2 value is 149 for 27 data points, corresponding to an average residuals about 2.3σ. That is to say this simple leptonic model actually can not fit the $HESS$ data well. This is a well-known result in previous studies (e.g., Aharonian et al. 2006; Tanaka et al. 2008; Morlino et al. 2009a; Fang et al. 2009). In Liu et al. (2008) the authors proposed a stochastic acceleration model to generate the electron spectrum with sub-exponential cutoff ($\delta_e = 0.5$) to better fit the $HESS$ data. However, in such a case the fit to X-ray data becomes worse. The X-ray data actually favors super-exponential cutoff instead (with $\delta_e = 1.2$ in this purely leptonic fit). The fit may be improved in some detailed leptonic models, as shown in Fan et al. (2010b), though systematic errors still dominate.

Table 1: Fitting parameters for $T_e = 10^7$ K. Errors are 1σ statistical uncertainties; limits correspond to 2σ confidence level.

	α_e	E_c^e (TeV)	W_e (10^{47}erg)	δ_e	B (μG)	$n_{\rm ISM}$ (10^{-2}cm^{-3})	α_p	E_c^p (TeV)	W_p (10^{52}erg)
leptonic	$2.15^{+0.01}_{-0.01}$	$51.3^{+2.3}_{-2.2}$	$5.5^{+0.3}_{-0.3}$	$1.21^{+0.04}_{-0.04}$	$11.6^{+0.1}_{-0.1}$	< 0.7	—	—	—
hadronic	$1.64^{+0.09}_{-0.08}$	$14.5^{+4.8}_{-3.9}$	$0.05^{+0.05}_{-0.02}$	$2.1^{+0.2}_{-0.2}$	$428.2^{+233.9}_{-159.6}$	< 1.1	$1.58^{+0.06}_{-0.06}$	$53.7^{+7.1}_{-6.2}$	> 1.6
hadronic*	$1.58^{+0.05}_{-0.05}$	$12.3^{+2.1}_{-1.8}$	$0.03^{+0.01}_{-0.01}$	$1.9^{+0.1}_{-0.1}$	$596.8^{+173.0}_{-129.0}$	< 1.2	—	$54.7^{+6.0}_{-5.7}$	> 1.4
hybrid	$2.14^{+0.01}_{-0.01}$	$50.7^{+2.1}_{-2.0}$	$4.6^{+0.3}_{-0.3}$	$1.23^{+0.04}_{-0.04}$	$12.0^{+0.2}_{-0.2}$	< 0.9	—	—	> 1.0

Table 2: Best-fit χ^2 values for each set of data and the total reduced one, for $T_e = 10^7$ K.

	radio	X-ray	GeV	TeV	reduced
leptonic	2.07	312.0	3.4	149.4	466.9/232
hadronic	0.13	291.7	1.9	40.6	334.4/229
hadronic*	0.10	291.9	1.9	40.5	334.4/230
hybrid	0.02	305.4	20.0	109.3	434.7/231

2.2. Hadronic scenario

In this subsection we discuss the model with a predominantly hadronic origin of the γ-rays. The spectrum of the accelerated protons is assumed to be $F_p(E) \propto E^{-\alpha_p} \exp[-(E/E_c^p)^{\delta_p}]$ with $\delta_p = 1$, which gives acceptable fit to the TeV data. The normalization is fixed using the total kinetic energy of protons with the energy $E > 1$ GeV. For the hadronic γ-ray production we adopt the parameterization of Kamae et al. (2006). With the additional three parameters, α_p, E_c^p, W_p, we have 9 parameters in total. Considering the synchrotron cooling[1] of high energy electrons, we also introduce a spectral break to the overall electron distribution[2]. The break energy, at which the synchrotron cooling time is equal to the lifetime of the remnant, is determined with $E_{\rm br} \approx 7.8 \times 10^6 (B/\mu{\rm G})^{-2} (T_{\rm life}/1600\,{\rm yr})^{-1}$GeV (Tanaka et al. 2008). For $E_e < E_{\rm br}$ the power-law index is α_e, and for $E_e > E_{\rm br}$ the power-law index is $\alpha_e + 1$. Since $T_{\rm life}$ is taken as 1600 years, $E_{\rm br}$ is not a free parameter.

The 1-D probability distributions and 2-D confidence contours of the model parameters, and the SED of the best-fit model are shown in Fig. 2. The parameters and χ^2 values of the best fit are listed in Tables 1 and 2, respectively. Still we adopt $T_e = 10^7$ K in this calculation. Compared with the leptonic model, a much stronger magnetic field is inferred, which is consistent with previous studies (Berezhko & Völk 2006) and the interpretation of the observed X-ray surface brightness fluctuations as synchrotron cooling of high energy electrons (Uchiyama et al. 2007). The 1-D probability distribution of most model parameters do not converge very well with multiple peaks except for those for α_p, and E_c^p, which are constrained by the γ-ray data directly, independent of other parameters in the hadronic scenario.

Due to the lack of constraint from the γ-ray data, the parameters related to electron emission can not be well determined with relatively large 1σ errors shown in Table 1, and there are strong correlations in the 2-D confidence contours, as shown in the middle panel of Fig. 2. The correlations among W_e, E_c^e, and B are due to the facts that the synchrotron emissivity $\epsilon \propto W_e B^2 E_c^{e2}$, and the high energy cutoff of synchrotron emission $\nu_c \propto B E_c^{e2}$. ν_c is well constrained by X-ray observations, which leads to the anti-correlation between B and E_c^e. The anti-correlation between W_e and B can be attributed to the measured luminosity of the synchrotron emission. The correlation between W_e and E_c^e results from these two anti-correlations. The strong anti-correlation between B and α_e is due to the radio to X-ray spectral shape, which, in combination with the anti-correlations between B and E_c^e, and B and W_e, leads to the correlations between α_e and E_c^e, and α_e and W_e, respectively. The correlations related to δ_e can be attributed to the hard X-ray spectrum. The weak correlation between α_p and E_c^p is due to the well-measured high-energy cutoff of the TeV emission. The strong anti-correlation between $n_{\rm ISM}$ and W_p is due to the fact that the product of $n_{\rm ISM}$ and W_p determines the hadronic component of γ-ray emission. Therefore we can get a lower limit of W_p according to the upper limit of $n_{\rm ISM}$. The 2σ upper limit of $n_{\rm ISM}$ is 0.01 cm^{-3}

---

[1] The IC cooling is negligible compared with the synchrotron cooling for magnetic fields greater than 10μG.

[2] The break energy in the leptonic (and the following hybrid) model is very high due to the weak magnetic field, and the electron spectrum is identical to a single power law.

for $T_e = 10^7$ K, corresponding to a lower limit of 1.6×10^{52} erg for W_p. The dependence of these results on T_e will be discussed in subsection 2.4. The constraint on W_p requires a total energy of CR protons much higher than typical energy output of a supernova explosion, say 10^{51} erg (Ellison et al. 2010; Zirakashvili & Aharonian 2010).

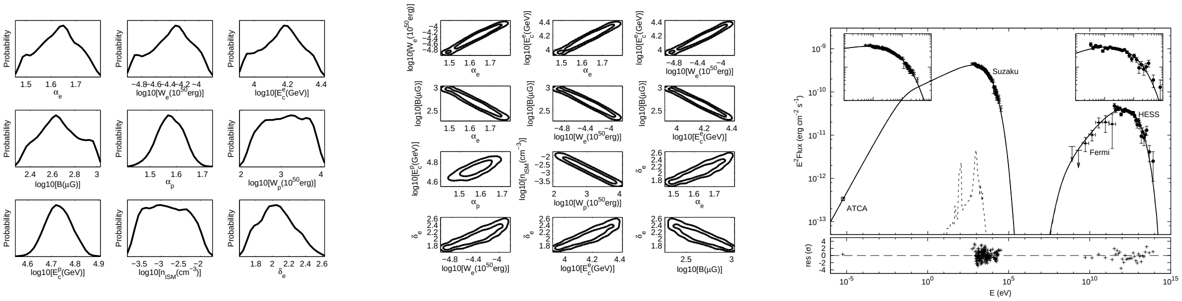

Fig. 2.— Same as Fig. 1 but for the hadronic scenario. The dashed line indicates the thermal emission for $T_e = 10^7$ K and $n_{\rm ISM} = 0.011$ cm^{-3}.

Table 2 shows clearly that the fits to GeV and TeV γ-ray data are significantly improved in the hadronic model. The average residual for the *HESS* data becomes $\sim 1.14\sigma$. The fit to the X-ray data also improves a bit due to a larger value of δ_e. Note, however, the reduced χ^2 of the global fit is about 1.46, which is still too large to be attributed to pure statistical errors. There are some systematical effects in either the data or the model. In particular, contributions to the χ^2 are dominated by the X-ray data in all these models, as shown in Table 2. It suggests that our simple one-zone synchrotron emission model does not give a sufficient description of the spatially integrated emission spectrum. Compared with the leptonic model, most reduction in the value of the χ^2 of the hadronic model comes from improved fit to the γ-ray data.

In the hadronic model the magnetic field is large, which suppresses the IC contribution to the γ-rays from energetic electrons and makes hadronic contribution to the γ-ray dominant. The strong magnetic field of the best fit model implies very efficient energy loss near the cutoff energy of electrons, which not only introduces a spectral break in the overall electron distribution but can also render the high energy cutoff sharper with $\delta_e = 2.1$ (Blasi 2010). It is interesting to note that the spectral index for electrons α_e is consistent with that for protons α_p, which is expected if the acceleration of these high-energy particles is due to the same physical process. The difference in their high-energy cutoffs can be attributed to the difference in the energy loss rate of protons and electrons near the cutoff energy. Therefore E_c^e should not be compared to E_e^p directly.

To reduce uncertainties of the model parameters in the hadronic scenario, we also consider the hadronic model with the constraint that $\alpha_e = \alpha_p$. The 1-D probability distribution and the 2-D confidence contours, and the best fit SED for such a model are shown in Fig. 3. Compared with Fig. 2, the probability distribution of the model parameters are better converged and the correlations in the 2-D confidence contours are weakened. The acceptable model parameter space is reduced significantly. The fitting results are also compiled in Tables 1 and 2 with a star mark. The value of the best fit model parameters agree with those of the hadronic model and the 1σ error of parameters related the electron emission are reduced significantly. The values of the χ^2 are essentially the same as the hadronic model.

The value of the spectral index for the best fit model is always much less than 2, a result difficult to accommodate with the diffusive shock model. This in combination with the low limit on W_p poses one of the most serious challenges to the hadronic scenario in the context of diffusive shock acceleration of SNRs. We also note that the best fit electron spectral index α_e is harder for the hadronic model than that for the leptonic model. Although the current radio data does not give a good constraint on synchrotron spectral index, a better measurement of the synchrotron spectrum in the future will be helpful in distinguishing these two scenarios for the TeV emission.

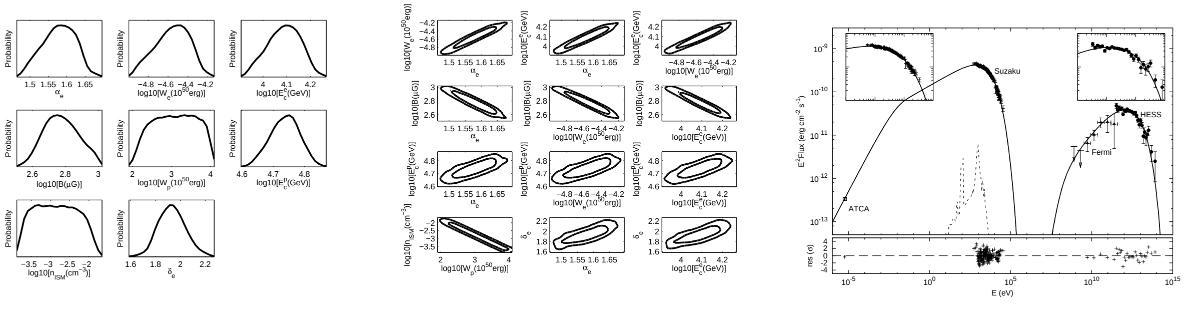

Fig. 3.— Same as Fig. 2 but for the hadronic scenario with the extra requirement of $\alpha_e = \alpha_p$.

2.3. Hybrid scenario

The results above agree with previous studies (Tanaka et al. 2008; Aharonian et al. 2006). They demonstrate clearly the strengths and problems associated with the leptonic and hadronic scenarios. The leptonic model has fewer parameters, most of which are well constrained with the MCMC method by fitting the SED. The fact that it can give reasonable good fits to the overall SED with reasonable values of the parameters may be considered as evidence for such a scenario (Fan et al. 2010a). On the other hand, the relatively high values of χ^2, especially for the γ-ray data, suggest that the model may not be complete. It has been shown that the TeV emission from SNR RX J1713.7-3946 may have significant contributions from energetic protons as well (Zirakashvili & Aharonian 2010; Katz & Waxman 2008).

However, in the most general case, at least three more parameters need to be introduced to characterize the distribution of accelerated protons, which leads to strong degeneracy of the model parameter space. And the challenges to the hadronic scenario, namely hard spectra of accelerated particles and the lower limit on W_p, does not appear to depend on this degeneracy in the regime of parameter space explored above.

In the subsection 2.2, we demonstrate that the acceptable model parameter space may be reduced significantly by considering some physically motivated constraint on the accelerated particle distributions. We have argued that the spectral indices of accelerated electrons and protons should be comparable in the relativistic energy regime where the energy loss can be ignored. In the hadronic scenario, due to the presence of strong magnetic field, there is a spectral break in the electron distribution and the high energy cutoffs of electrons and protons do not need to be the same. However, in the leptonic scenario, the magnetic field is so weak that the energy loss does not affect the distribution of both electrons and protons. For these high energy relativistic electrons and protons, their gyro-radius only depends their energy and the magnetic field. We would expect that mechanisms of charged particle acceleration will lead to identical particle distributions except their normalization, which is determined by different injection processes at low energies (Petrosian & Liu 2004). To reduce the number of model parameters, one may therefore consider the hybrid scenario where $\alpha_e = \alpha_p$, $\delta_e = \delta_p$, and $E_c^e = E_c^p$. As we will show below, this leads to a hybrid explanation to the high energy γ-ray data. The total number of free parameters in the hybrid model is now only 7.

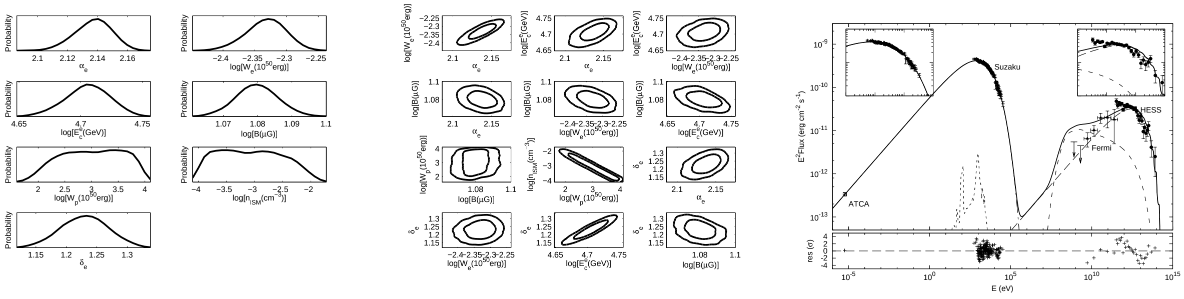

Fig. 4.— Same as Fig. 1 but for the hybrid scenario. The density for the thermal emission indicated by the dashed line is 0.009 cm^{-3}.

The model parameter distributions and best-fit SED are shown in Fig. 4. The background electron temperature is still adopted as 10^7 K. The best fit results and χ^2 values are also listed in Tables 1 and 2. We see that the parameters of the electron component do not change significantly compared with the leptonic scenario primarily due to the dominance of TeV emission by relativistic electrons through the IC process. The hadronic component dominates the GeV γ-ray emission. Note that since $E_c^p = E_c^e$, the γ-ray spectrum of the hadronic component cuts off at a lower energy than the leptonic component. Neutral pion decays into two γ-ray photos. The cutoff energy of the γ-ray spectrum is at least a factor of 2 lower than the cutoff energy of the corresponding proton distribution. For the IC emission, the cutoff energy of the γ-ray spectrum can be the same as the corresponding electron distribution. The fit to TeV data shows improvement compared with the leptonic model, with average residual changing from $\sim 2.3\sigma$ to about 2.0σ. However, the hadronic component seems to overproduce the GeV flux, resulting in an even larger $\chi^2_{\rm GeV}$ than the leptonic scenario. The χ^2 value for X-ray data does not change significantly. The correlation of the model parameters are also similar to the leptonic model. And the strong anti-correlation between $n_{\rm ISM}$ and W_p is still due to the fact that the observed emission is determined by the product of the two. Although the model has a weak magnetic field and relatively soft distributions of accelerated particles, the 2σ lower limit of the proton energy of 1.0×10^{52} ergs is comparable to those of the hadronic models, which still challenges the energetics of the SNR.

2.4. Dependence of T_e

The energy content of relativistic protons is poorly determined due to the high uncertainty in $n_{\rm ISM}$. Perhaps the only observation one can use to constrain $n_{\rm ISM}$ is the lack of thermal X-ray emission from the remnant (Cassam-Chenaï et al. 2004). To derive a robust constraint on $n_{\rm ISM}$, one however needs to consider the heating of electrons and the ionization of ions in the background plasma, both of which are not well understood though a preliminary attempt has been taken to model these processes quantitatively (Ellison et al. 2010). Here we assume that electrons have reached ionization equilibrium with the ions and so that the Raymond-Smith code can be used to calculate the thermal emission.

The results above do not differ significantly for different values of T_e except for the constraint on $n_{\rm ISM}$ and accordingly W_p. In Fig. 5 we show the results for the hybrid scenario with $T_e = 10^6$ and 10^8 K. For $T_e = 10^6$ K most of the line emission has energies lower than 0.5 keV, which is below the lower limit of the *Suzaku* data. However, the emission in the X-ray band is sufficient to lead to well-constrained $n_{\rm ISM} \sim 0.2$ cm^{-3} and $W_p \sim 10^{51}$ ergs. The model also predicts strong emission below the X-ray range. A significant thermal component also helps to slightly improve the fit to the X-ray data. The 2σ upper limit of $n_{\rm ISM}$ for $T_e = 10^6$ K is 0.2 cm^{-3}, which is much looser than that for $T_e = 10^7$ K. For $T_e = 10^8$ K the 2σ upper limit of $n_{\rm ISM}$ is 0.02 cm^{-3}, which is also higher than 0.009 cm^{-3} for $T_e = 10^7$ K. The 2σ lower limits of W_p are 3.5×10^{50}, 1.0×10^{52}, and 4.4×10^{51} ergs for $T_e = 10^6$, 10^7, and 10^8 K respectively.

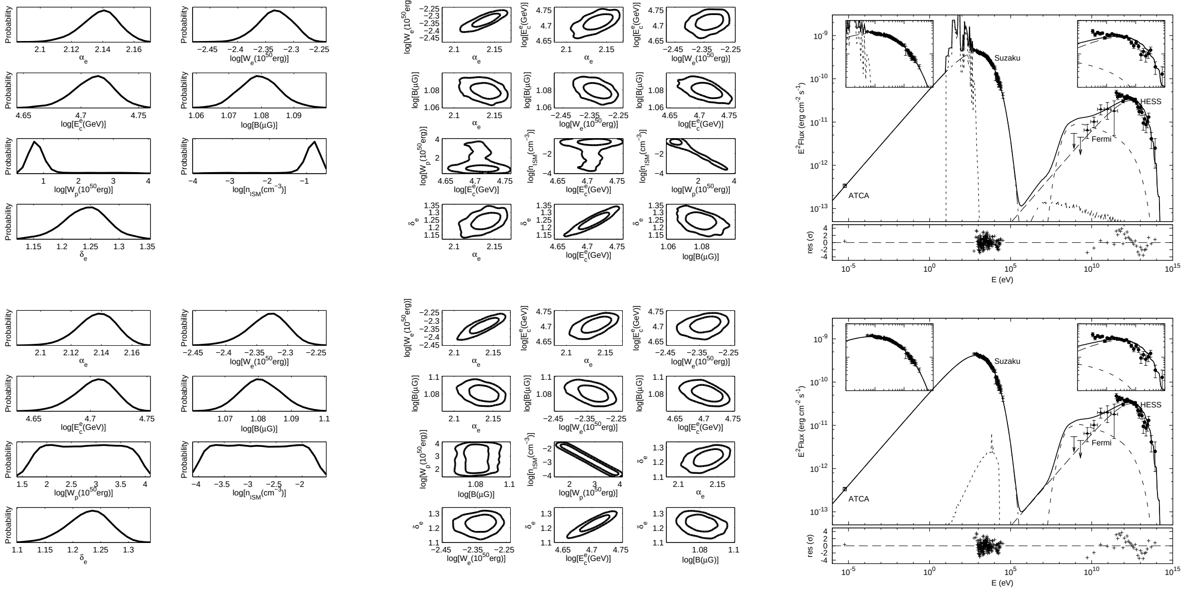

Fig. 5.— Same as Fig. 4 but for two other background electron temperatures: 10^6 (upper) and 10^8 (lower) K. The corresponding density $n_{\rm ISM}$ for the thermal emission is 0.2 cm^{-3} (upper) and 0.02 cm^{-3} (lower).

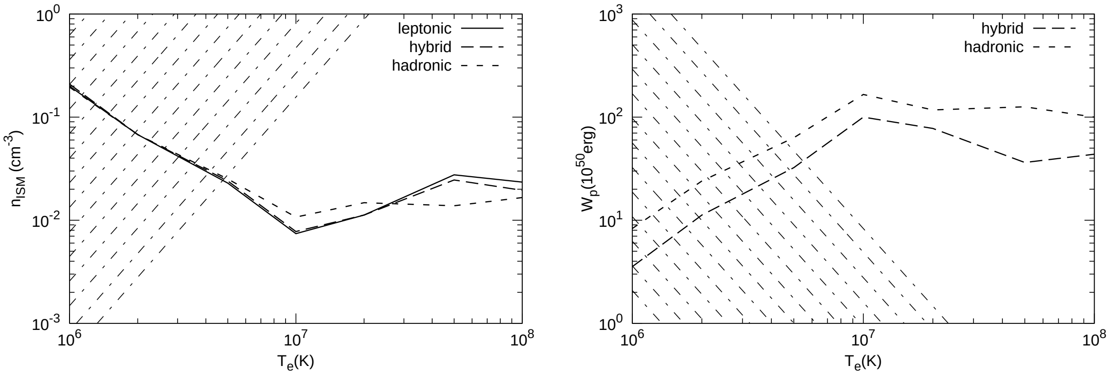

Fig. 6.— The 2σ upper limits of $n_{\rm ISM}$ (left) and lower limits of the energy content of non-thermal protons W_p (right) as functions of the temperature of background electrons T_e for different models. The shaded region can be excluded due to heating of electrons by background protons through Coulomb collisions.

To demonstrate how the constraint on $n_{\rm ISM}$ and W_p vary with T_e, we repeat the MCMC calculation for a series of T_e. The 2σ upper limit of $n_{\rm SIM}$ and lower limit of W_p are shown in Fig. 6. In the left panel the constraints on $n_{\rm ISM}$ of the three scenarios are shown, while in the right panel the constraints on W_p are relevant for the hybrid and hadronic models.

The constraints on $n_{\rm ISM}$ are almost the same for the leptonic and hybrid models since their parameters for the synchrotron emission are similar. For the hadronic model the result is slightly different primarily due to difference in the electron distribution. The lower limit on W_p for the hybrid scenario is a bit smaller than the hadronic model because in the hybrid model the IC component from the lepton population has a significant contribution to the γ-ray. The shaded region in the left panel is excluded by considering the heating of electrons by ions through Coulomb collisions with the scaling relation of Eq. (1). In the right panel the shaded region is derived by applying the relation $W_p/10^{50}\,{\rm erg} \sim 1.3\,{\rm cm}^{-3}/n_{\rm ISM}$, which is the approximate relation required to reproduce the high energy γ-ray emission for the hybrid and hadronic scenarios. It can be seen that in general W_p needs to be greater than $\sim 4 \times 10^{51}$ erg for the hybrid model. For the hadronic scenario the requirement of W_p is even larger. Such a large value of proton energy seems to be unacceptably high for a typical SNR (Ellison et al. 2010; Zirakashvili & Aharonian 2010). The 2σ upper limit of $n_{\rm ISM}$ is less than 0.03 $\rm cm^{-3}$, which is consistent with that obtained by Cassam-Chenaï et al. (2004) from *XMM-Newton* observations.

3. Discussion and Conclusion

Since the discovery of synchrotron X-ray emission from the forward shock of SN 1006 (Koyama et al. 1995), it has been established that shocks of SNRs can accelerate electrons to tens of TeV. The detection of TeV emission directly from a few shell type SNRs confirmed this conclusion (Lazendic et al. 2004; Aharonian et al. 2005, 2008). However, the nature of the TeV emission is still a matter of debate. X-ray observations also reveal strong thermal emission in the interior of a few young SNRs. Thermal X-ray emission from the forward shock, on the other hand, is usually weak and only detected in relatively old remnants, such as RCW 86 (Vink et al. 2006). Since the observed TeV emission is well correlated with the forward shock, the lack of thermal X-ray emission implies low gas density and therefore high energy content of accelerated protons in the hadronic model for the TeV emission, which is difficult to accommodate with the SNR theories. The leptonic model in general gives a poorer fit to the TeV spectrum than the hadronic model. More detailed modeling is necessary to distinguish these emission models.

Using the MCMC method, we systematically investigate the parameter space of models for the multi-wavelength emission of SNR RX J1713.7-3946. The high quality of observational data, especially X-ray data from *Suzaku* and TeV γ-ray data from $HESS$, enables us to get very good constraints on most model parameters and better understand the emission mechanisms. The radio and X-ray emissions are thought to be produced by the synchrotron radiation of relativistic electrons accelerated in the SNR. The high energy γ-ray emission (from GeV to TeV) can be produced through the IC radiation of electrons scattering off background low energy photons, and/or the decay of π^0 generated through CR proton-ISM collisions. We study three kinds of scenarios, the leptonic one, hadronic one and a hybrid one, distinguished through the emission mechanism of high energy γ-rays. Thermal emissions, including continuous and line emissions, are included in the modeling to constrain density of the background plasma with the absence of thermal emission in X-ray observations.

The global fit of these three scenarios shows that: 1) the goodness-of-fit is the worst for the leptonic model and the best for the hadronic model; 2) the X-ray data can set an upper limit on the background ISM density, which is $0.03 - 0.009$ cm^{-3} depending on the temperature of the background electrons; 3) the upper limit of $n_{\rm ISM}$ leads to a lower limit of energy content of relativistic protons $W_p > 4 \times 10^{51}$ (6×10^{51}) erg for the hybrid (hadronic) model, which seems to be too high for a typical core-collapse supernova. The well constrained parameters of the leptonic scenario are more physically acceptable, although the hybrid and hadronic scenarios give smaller χ^2 values. In some physically motivated models of electron acceleration in SNR, the goodness-of-fit can be improved (Fan et al. 2010b), and our overall results appear to favor the leptonic scenario (Ellison et al. 2010). However, systematic errors in the X-ray and TeV band are significant in all the emission models studied so far, which demands more advanced modeling. For example, the observed source structure is much richer than the simple uniform zone assumed in all the emission models. On the other hand, given difficulties in X-ray and TeV observations, the errors of the relevant data may also be underestimated, especially the *HESS* fluxes at the low energy range, which does not appear to smoothly match the recently obtained GeV fluxes with the *Fermi* observatory (Abdo et al. 2011).

In the following we discuss several possible alternatives of the hadronic scenario, in order to provide an independent judge of the price needed to pay to keep the hadronic model working. The most serious challenge to the hadronic and hybrid models is the high energy content of relativistic protons inferred from the upper limit of the background density. This high energy content is in excess of typical supernova explosions, but could be explained by hypernovae. The total kinetic energy of the SNR with a shock speed U may be estimated as

$$K = \frac{2\pi}{3} R^3 n_{\rm ISM} m_p U^2 \simeq 6 \times 10^{50} \left(\frac{R}{10\ \rm pc}\right)^3 \left(\frac{U}{4500\ \rm km/s}\right)^2 \left(\frac{n_{\rm ISM}}{0.03\ \rm cm^{-3}}\right) \rm ergs.$$

With the current best estimate of the distance at 1 kpc, the radius of the remnant is 10 pc. For such a remnant size, the total kinetic energy content (K) of the remnant is much less than typical hypernovae and less than the energy content of relativistic protons. However, the distance to the SNR is not well determined. The lack of thermal X-ray emission directly constrains the integration along the line-of-sight of the thermal emissivity, which is proportional to $n_{\rm ISM}^2 R$. The radius R and shock speed U of the SNR scales linearly with the distance D. The upper limit on $n_{\rm ISM}$ therefore is proportional to $D^{-1/2}$; K is proportional to $D^{9/2}$. The γ-ray flux produced via hadronic process is proportional to $W_p n_{\rm ISM}/D^2$. The lower limit on W_p therefore is proportional to $D^{5/2}$. The total kinetic energy of the SNR decreases more rapidly than W_p, making the discrepancy between these two energies worse for shorter distance D. An increase of D by a factor of 3, on the other hand, can make the upper limit on W_p less than K, which is now $\sim 8\times 10^{52}$ erg, at the high end of observed hypernovae (Nomoto et al. 2005). This may explain the rareness of this kind of shell type TeV SNRs with non-detection of thermal X-ray emission. For the few tens of SNRs observed in X-rays, two of them show complete absence of thermal emission (Vink 2006). The efficiency of proton acceleration also needs to be greater than 50% for this model to work (Helder et al. 2009). The upper limit on the density is then about 0.02 $\rm cm^{-3}$, which is not too different from values obtained above and from previous studies.

Alternatively, the hadronic and hybrid models can work by overcoming the upper limit on the ISM density placed by the upper limit on the thermal electron emission. This limit arises from using the standard ion-electron coupling term from Hughes et al. (2000) producing a lower limit on the electron temperature (Eq. (1)). But this assumed a standard profile for the remnant. If the emission of this remnant is instead produced by the interaction of the supernova shock striking a thin shell of material ejected from the star prior to collapse (e.g. an outburst from a luminous blue variable or binary mass ejection), the electrons might still be cold. However, to do so would require very fine-tuned arguments (for the electron temperature to be below 2×10^6K, the shock must have hit the stellar ejecta less than 25 yr ago). Even with this fine-tuning, this thin shell of material would not have a large enough emitting volume to explain the observed high-energy emission. A thin shell explanation seems unlikely. It was also suggested that the effective particle acceleration would make the post-shock medium be less heated (Drury et al. 2009), however, the extreme condition in such a scenario seems difficult to satisfy, and the non-linear effects will also make the medium be heated more significantly (Ellison et al. 2010).

A plausible explanation of the low inferred density of the background plasma is the assumption of ionization equilibrium adopted in calculating the thermal emission, which however may not be valid. For the case with a large fraction of neutral medium, $n_e \ll n_{\rm ISM}$, the constraint on $n_{\rm ISM}$ from the thermal emission, which is proportional to $n_e n_{\rm ISM}$, will be much weaker than the case with fully ionized gas. Therefore the requirement of W_p can be smaller and the difference between W_p and the power of typical supernova can be reduced. In such a case, the low density of ionized ISM implies that neutral gases can penetrate a depth of

$$6 \times 10^{17} \left(\frac{n_{\rm ISM}}{0.03\ {\rm cm}^{-3}}\right) \left(\frac{U}{4500{\rm km/s}}\right) \left(\frac{T_e}{10^7{\rm K}}\right)^{0.23} {\rm cm}$$

before being ionized by the free electrons (Chevalier & Raymond 1978). For very low density of ionized plasma in the shocked downstream region, this depth can be a significant fraction of the radius of the remnant, and one may expect strong H_α emissions (Ghavamian et al. 2007; Helder et al. 2009). Better treatment of the ionization balance in the shock downstream may address this issue.

Finally we mention that neutrino signal can be used to test the hybrid/hadronic model of the γ-ray emission. It is shown that if the TeV γ-rays are predominantly produced by hadronic interactions, the accompanied neutrino signal might be detected in the up-coming km^3 neutrino detector, such as KM3NET (Kistler & Beacom 2006; Yamazaki et al. 2009; Morlino et al. 2009b; Yuan et al. 2010).

The MCMC code is adapted from the COSMOMC package (Lewis & Bridle 2002). QY thanks Jie Liu for the help to develop the code. This work is supported in part by the Natural Sciences Foundation of China (Nos. 10773011, 10963004, 11075169 and 11143007), the 973 project under the grant No. 2010CB833000, the Yunnan Provincial Science Foundation of China under the grant No. 2008CD061, a Marie Curie research fellowship at the University of Glasgow, and, under the auspices of the National Nuclear Security Administration of the U.S. Department of Energy at Los Alamos National Laboratory, supported by Contract No. DE-AC52-06NA25396.

REFERENCES

Abdo, A. et al. 2011, arXiv:1103.5727

Acero, F., Ballet, J., Decourchelle, A., Lemoine-Goumard, M., Ortega, M., Giacani, E., Dubner, G. & Cassam-Chenaï, G. 2009, A&A, 505, 157

Aharonian, F. et al. 2004, Nature, 432, 75

Aharonian, F. et al. 2005, A&A, 437, L7

Aharonian, F., et al. 2006, A&A, 449, 223

Aharonian, F., et al. 2007, A&A, 464, 235

Aharonian, F., et al. 2008, ApJ, 692, 1500

Allen, C. W. 1973, Astrophysical quantities (London: University of London, Athlone Press)

Axford, W. I. 1981, in International Cosmic Ray Conference, Vol. 12, 155

Benjamin, R. A., et al. 2003, PASP, 115, 953

Berezhko, E. G. & Ellison, D. C. 1999, ApJ, 526, 385

Berezhko, E. G. & Völk, H. J. 2006, A&A, 451, 981

Berezhko, E. G. & Völk, H. J. 2010, A&A, 511, A34

Blasi, P. 2010, MNRAS, 402, 2807

Butt, Y. M., Porter, T. A., Katz, B., & Waxman, E. 2008, MNRAS, 386, L20

Cassam-Chenaï, G., Decourchelle, A., Ballet, J., Sauvageot, J. L., Dubner, G. & Giacani, E. 2004, A&A, 427, 199

Chevalier, R. A. & Raymond, J. C. 1978, ApJ, 225, L27

Drury, O'C., Aharonian, F. A., Malyshev, D., & Gabici, S. 2009, A&A, 496, 1

Ellison, D. C., Patnaude, D. J., Slane, P., & Raymond, J. 2010, ApJ, 712, 287

Enomoto, R., et al. 2002, Nature, 416, 823

Fan, Z., Liu, S., & Fryer, C. L. 2010a, MNRAS, 406, 1337

Fan, Z. H., Liu, S. M., Yuan, Q., & Fletcher, L. 2010b, A&A, 517, L4

Fang, J., Zhang, L., Zhang, J. F., Tang, Y. Y., & Yu, H. 2009, MNRAS, 392, 925

Gamerman, D. 1997, Markov Chain Monte Carlo: Stochastic Simulation for Bayesian Inference (Chapman and Hall, London)

Ghavamian, P., Laming, J. M., & Rakowski, C. E. 2007, ApJ, 654, L69

Gabici, S. 2008, arXiv:0811.0836

Helder, E. A., et al. 2009, Science, 325, 719

Hughes, J. P., Rakowski, C. E., & Decourchelle, A. 2000, ApJ, 543, L61

Kamae, T., Karlsson, N., Mizuno, T., Abe, T., & Koi, T. 2006, ApJ, 647, 692

Katz, B. & Waxman, E. 2008, J. Cosmology Astropart. Phys., 1, 18

Kistler, M. D. & Beacom, J. F. 2006, Phys. Rev. D, 74, 063007

Koyama, K., Petre, R., Gotthelf, E. V., Hwang, U., Matsuura, M., Ozaki, M. & Holt, S. S. 1995, Nature, 378, 255

Koyama, K., Kinugasa, K., Matsuzaki, K., Nishiuchi, M., Sugizaki, M., Torii, K., Yamauchi, S. & Aschenbach, B. 1997, PASJ, 49, L7

Koyama, K., et al. 2007, PASJ, 59, 23

Lazendic, J. S., Slane, P. O., Gaensler, B. M., Reynolds, S. P., Plucinsky, P. P. & Hughes J. P. 2004, ApJ, 602, 271

Lewis, A. & Bridle, S. 2002, Phys. Rev. D, 66, 103511

Liu, S., Fan, Z., Fryer, C. L., Wang, J., & Li, H. 2008, ApJ, 683, L163

Mackay, D. J. C. 2003, Information Theory, Inference and Learning Algorithms (Cambridge University Press)

Morlino, G., Amato, E., & Blasi, P. 2009a, MNRAS, 392, 240

Morlino, G., Blasi, P., & Amato, E. 2009b, Astroparticle Physics, 31, 376

Moskalenko, I. V., Porter, T. A., & Strong, A. W. 2006, ApJ, 640, L155

Muraishi, H., et al. 2000, A&A, 354, L57

Neal, R. M. 1993, Probabilistic Inference Using Markov Chain Monte Carlo Methods (Department of Computer Science, University of Toronto)

Nomoto, K., Maeda, K., Tominaga, N., Ohkubo, T., Deng, J. & Mazzali, P. 2005, Ap&SS, 298, 81

Petrosian, V. & Liu, S. 2004, ApJ, 610, 550

Plaga, R. 2008, New Astronomy, 13, 73

Porter, T. A., Moskalenko, I. V., & Strong, A. W. 2006, ApJ, 648, L29

Raymond, J. C. & Smith, B. W. 1977, ApJS, 35, 419

Tanaka, T., et al. 2008, ApJ, 685, 988

Uchiyama, Y., Aharonian, F. A., & Takahashi, T. 2003, A&A, 400, 567

Uchiyama, Y., Aharonian, F. A., Tanaka, T., Takahashi, T., & Maeda, Y. 2007, Nature, 449, 576

Vink, J. 2006, arXiv:astro-ph/0601131

Vink, J., Bleeker, J., van der Heyden, K., Bykov, A., Bamba, A. & Yamazaki, R. 2006, ApJ, 648, L33

Wang, Z. R., Qu, Q., & Chen, Y. 1997, A&A, 318, L59

Warren, J. S., et al. 2005, ApJ, 634, 376

Yamazaki, R., Kohri, K., & Katagiri, H. 2009, A&A, 495, 9

Yuan, Q., Yin, P., & Bi, X. 2010, ArXiv e-prints:1010.1901

Zirakashvili, V. N. & Aharonian, F. A. 2010, ApJ, 708, 965

This preprint was prepared with the AAS LaTeX macros v5.2.